Multicomponent Donor−Acceptor Relay System Assembled within the Cavities of Zeolite Y. Photoinduced Electron Transfer between $Ru(bpy)_3^{2+}$ and 2,4,6-Triphenylpyrylium in the Presence of Interposed TiO_2

Mercedes Álvaro,[†] Michelle N. Chrétien,[‡] Vicente Fornés,[†] María S. Galletero,[†] Hermenegildo García,*[,‡] and J. C. Scaiano*[,†]

Instituto de Tecnología Química CSIC-UPV, Universidad Politécnica de Valencia, Apartado 22012, 46071-Valencia, Spain, and Department of Chemistry, Centre for Catalysis Research and Innovation, University of Ottawa, K1N 6N5 Ottawa, Canada

Received: February 3, 2004; In Final Form: June 9, 2004

Zeolite Y containing $Ru(bpy)_3^{2+}$ and TP^+ has been obtained by the stepwise ship-in-a-bottle synthesis of the two components. The identity of the two ions has been demonstrated by diffuse reflectance UV−vis and IR spectra. Emission spectra ($\lambda_{ex} = 466$ nm, $\lambda_{em} = 600$ nm) corresponding to the $Ru(bpy)_3^{2+}$ lumophore indicate that 70% of the $Ru(bpy)_3^{2+}$ complexes interact with TP^+ through static quenching; only a weak emission corresponding to the unquenched complex is observed. The transient absorption spectrum of $[Ru(bpy)_3^{2+}-TP^+]$@Y obtained by laser flash photolysis is complex, but the presence of $Ru(bpy)_3^{3+}$ was detected. The co-incorporation of semiconductor oxide TiO_2 disfavors the $Ru(bpy)_3^{2+}-TP^+$ interaction, restoring the $Ru(bpy)_3^{2+}$ emission to 90% of the original value. This indicates that small TiO_2 clusters of a few Ti atoms occupying the empty zeolite space (1.3 nm) and, having a much larger band gap than regular TiO_2, (∼50 nm) act mainly as insulators between good electron donor and acceptor molecules as opposed to electron relays.

Introduction

Numerous studies have dealt with photoinduced electron transfer (PET) between various donor (D) and acceptor (A) molecules within zeolite Y cavities.[1−17] In this process, it is frequently assumed that the zeolite plays a "passive" role, simply providing a highly polar environment favoring electron transfer.[11,18−20] One common observation is a remarkable increase in the lifetime of the charge-separated species as compared to that of the same system in solution.

$Ru(bpy)_3^{2+}$ is often employed as an electron donor in studies of intrazeolite PET, frequently in combination with viologens as the electron acceptor.[12,13,16,21−31] In this report, we describe the intrazeolite PET interaction between $Ru(bpy)_3^{2+}$ (D) and 2,4,6-triphenylpyrylium (TP^+, A) in the absence or presence of semiconductor oxide clusters (TiO_2) interposed in the "intracrystalline" space between them. In the absence of TiO_2, the zeolite interior is occupied by coadsorbed water molecules. Both $Ru(bpy)_3^{2+}$ and TP^+ are large molecules that cannot be accommodated by the ∼7.4-Å cavity windows and must be prepared by ship-in-a-bottle synthesis. Because of these size constraints, there is no possibility of either doubly occupied cavities or guest migration through the zeolite micropores. The closest D−A distance therefore corresponds to neighboring supercages. This immobility is in contrast to previous studies employing mobile viologen molecules as electron acceptors. We have attempted to modulate the D−A interaction by modifying the intracrystalline space between them. The zeolite voids have been modified with semiconducting oxide (TiO_2) clusters, whose role affecting the electron transfer between D and A either as electron relays or insulators is unclear from the literature, particularly considering that the small size of the intracrystalline TiO_2 cluster considerably increases the band gap between the valence and the conduction band with respect to typical P-25 TiO_2 standard particles (∼50 nm). The aim of this work is to understand the influence of the interposed semiconductor medium on intrazeolite PET.

SCHEME 1: $Ru(bpy)_3^{2+}$ and TP^+ Immobilized Inside Separated Zeolites Cavities

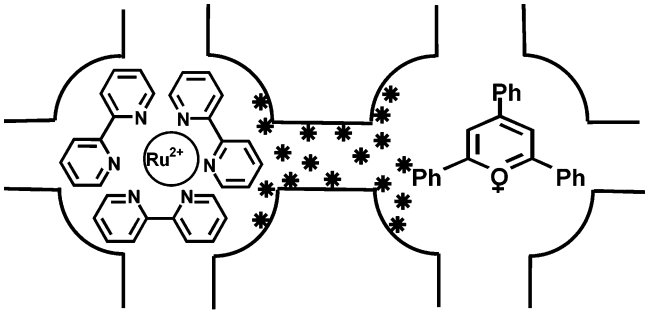

Results and Discussion

The samples examined in this study contained both $Ru(bpy)_3^{2+}$ and TP^+. The preparation of $Ru(bpy)_3^{2+}$ or TP^+, separately encapsulated inside zeolite Y, by ship-in-a-bottle synthesis has been previously reported in the literature.[31−34] The current samples were prepared in a stepwise fashion; $Ru(bpy)_3^{2+}$ was first encapsulated according to literature procedures,[35] and co-encapsulated TP^+ was prepared by the thermal cyclization of adsorped 1,3,5-triphenyl-2-penten-1,5-dione.[36] Scheme 2 outlines the preparation of $[Ru(bpy)_3^{2+}-TP^+]$@Y. (See Experimental Section for details.) This sequence, the preparation

* Corresponding authors. E-mail: hgarcia@qim.upv.es.
† Universidad Politécnica de Valencia.
‡ University of Ottawa.

10.1021/jp049520x CCC: $27.50
Published on Web 10/01/2004

TABLE 1: Relevant Analytical and Spectroscopic Data of the Samples Studied

samples	DR λ_{max} (nm)	combustion analyses (C, H, N)/Ti(%)	IR (cm^{-1}) characteristic peaks
$[Ru(bpy)_3^{2+}-TiO_2-TP^+]$@Y (0.9)	285, 329, 420, 460	Ti: 0.9 N: 2.82 C: 11.27 H: 2.35	TP^+: 1626, 1595, 1576, 1491
$[Ru(bpy)_3^{2+}-TiO_2-TP^+]$@Y (1.8)		Ti: 1.8 N: 2.92 C: 12.27 H: 2.45	$Ru(bpy)_3^{2+}$: 1607, 1465, 1450, 1427
$[Ru(bpy)_3^{2+}-TP^+]$@Y	290, 400	N: 2.96 C: 12.07 H:2.12	TiO_2: 1693
$[Ru(bpy)_3^{2+}-TiO_2]$@Y	250, 440, 456	N: 2.34 C: 9.56	

SCHEME 2: Preparation of Sample $[Ru(bpy)_3^{2+}-TP^+]$@Y

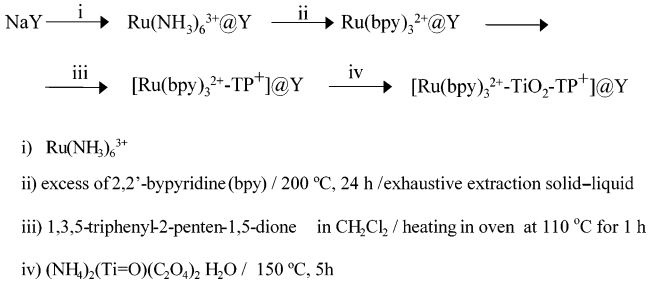

of $Ru(bpy)_3^{2+}$ followed by the formation of TP^+, was preferable given that the conditions for the preparation of TP^+ are mild and compatible with the presence of $Ru(bpy)_3^{2+}$. The preparation of TP^+ followed by $Ru(bpy)_3^{2+}$ could result in the decomposition of TP^+ because of the prolonged heating (24 h at 200 °C) required for the synthesis of $Ru(bpy)_3^{2+}$.

$[Ru(bpy)_3^{2+}-TP^+]$@Y was subjected to a consecutive synthesis step in order to incorporate TiO_2 clusters. The preparation of TiO_2 clusters inside zeolites has also been reported.[12,30,37−48] To form TiO_2 clusters inside $[Ru(bpy)_3^{2+}-TP^+]$@Y, $Ti{=}O^{2+}$ was introduced via ion exchange, followed by thermal oligomerization at 150 °C.[30] This is shown in Scheme 2. (see Experimental Section for details.)

We have also studied samples of $Ru(bpy)_3^{2+}$@Y and $[Ru(bpy)_3^{2+}-TiO_2]$@Y in which the electron-acceptor component (TP^+) was not present. Table 1 summarizes the samples under study and their main analytical and spectroscopic data. Each sample contained the same loading of $Ru(bpy)_3^{2+}$, estimated as 1 complex per 6 supercages as determined by an analysis of ruthenium and nitrogen. A comparison of the carbon and nitrogen content before and after the synthesis of TP^+ indicates that the TP^+ loading is approximately 1 cation every 2.5 supercages. As a result of the sequential synthetic procedure, samples that differ in the nature of the internal medium (i.e., 0, 0.9, and 1.8% TiO_2) each contain the same loading of $Ru(bpy)_3^{2+}$ and TP^+.

The influence of TiO_2 is likely to be more remarkable at high loadings. To achieve this, it was necessary to proceed through two consecutive ion-exchange cycles. For this reason, Table 1 lists two TiO_2-containing samples, 0.9 and 1.8, which were obtained by one or two ion-exchange cycles of the titanyl salt. Evidence for the internal location of TiO_2 is derived from transmission electron microscopy that does not show the presence of independent TiO_2 and from the remarkable band-gap shift of TiO_2 as compared to the regular P-25 TiO_2 standard. The TiO_2 content is limited by the intracrystalline space available as well as by diffusion restrictions imposed by the presence of preexisting $Ru(bpy)_3^{2+}$ and TP^+.

The concurrent presence of $Ru(bpy)_3^{2+}$ and TP^+ was assessed using various spectroscopic methods. The diffuse reflectance UV−vis spectrum of the $[Ru(bpy)_3^{2+}-TP^+]$@Y sample shows a broad band corresponding to an envelope of the two chromophores (Figure 1), but the peaks characteristics of each cation ($Ru(bpy)_3^{2+}$ λ_{abs} = 460 nm, TP^+ λ_{abs} = 370, 420 nm) could not be resolved.

Considerably more information concerning the presence of $Ru(bpy)_3^{2+}$ and TP^+ was obtained by IR spectroscopy. In the IR spectrum of $[Ru(bpy)_3^{2+}-TP^+]$@Y, the characteristic vibration bands corresponding to $Ru(bpy)_3^{2+}$ and TP^+ could be concurrently observed. Figure 2 shows that the IR spectrum of $[Ru(bpy)_3^{2+}-TP^+]$@Y is actually a combination of that for $Ru(bpy)_3^{2+}$@Y and TP^+@Y.

The emission from $[Ru(bpy)_3^{2+}-TP^+]$@Y was recorded upon excitation with wavelengths in the range from 420 to 490 nm, and the emission was mapped as a function of the excitation wavelength. Figure 3 shows the clear variation in λ_{em} depending

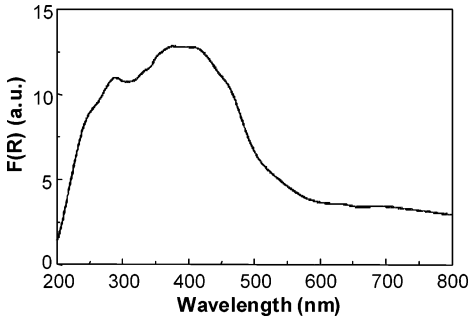

Figure 1. Diffuse reflectance UV−vis spectrum (plotted as the Kubelka−Munk function of the reflectance, F(R)) of $[Ru(bpy)_3^{2+}-TP^+]$@Y.

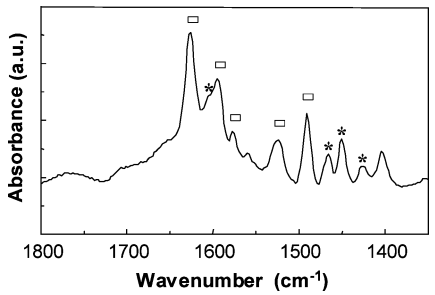

Figure 2. Aromatic region of the FT-IR spectrum recorded for $[Ru(bpy)_3^{2+}-TP^+]$@Y after heating at 200 °C under 10^{-2} Pa for 1 h. The characteristic peaks corresponding to $Ru(bpy)_3^{2+}$ (*) and TP^+ (□) have been labeled.

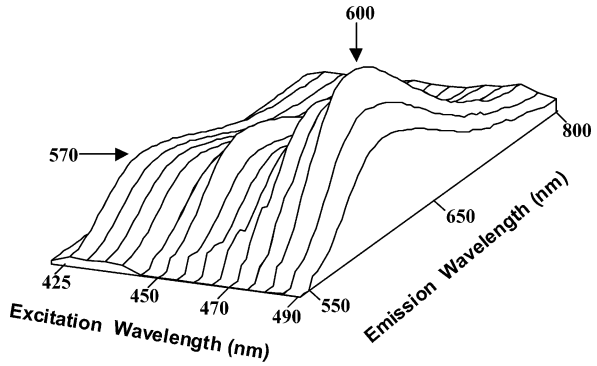

Figure 3. Map of the emission spectra as a function of the excitation wavelength in the range 420−490 nm for [Ru(bpy)$_3^{2+}$−TP$^+$]@Y under N_2.

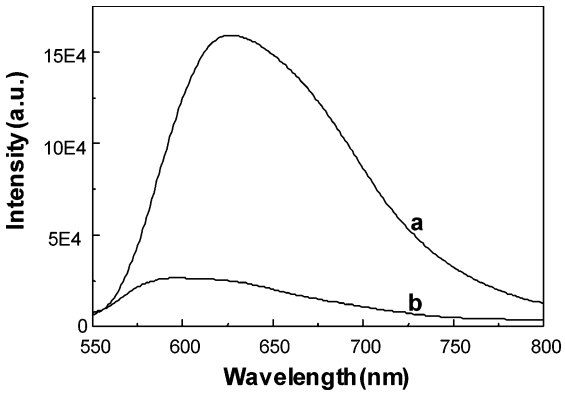

Figure 4. Average emission spectrum (λ_{ex} = 466 nm) for samples (a) Ru(bpy)$_3^{2+}$@Y and (b) [Ru(bpy)$_3^{2+}$−TP$^+$]@Y. Each of these spectra is an average of nine independent measurements.

on the excitation wavelength. The collected spectra can be interpreted as a combination of variable proportions of the emission arising from TP$^+$ and/or Ru(bpy)$_3^{2+}$; the emission of Ru(bpy)$_3^{2+}$ (λ_{em} = 600 nm) is significantly different from that of TP$^+$ (λ_{em} = 570 nm). In a sample containing both species, the emission of either TP$^+$ or Ru(bpy)$_3^{2+}$ can be preferentially observed depending on the excitation wavelength; for example, excitation at 480 nm results in emission almost exclusively corresponding to Ru(bpy)$_3^{2+}$. In subsequent work, we have primarily utilized emission from Ru(bpy)$_3^{2+}$ with the expectation that the longer emission wavelength would minimize possible interference due to emission-reabsorption phenomena.

Previous reports in the literature have made ample use of Ru(bpy)$_3^{2+}$ emission to study its interaction with quenchers in zeolitic media.[18,49,50] In the present case, a comparison of emission spectra for the Ru(bpy)$_3^{2+}$@Y sample before and after incorporation of TP$^+$ shows a significant intensity decrease corresponding to 70% of the original emission (Figure 4). The lifetime of the emission was also monitored at 600 nm for both Ru(bpy)$_3^{2+}$@Y and [Ru(bpy)$_3^{2+}$−TP$^+$]@Y. As can be seen in Figure 5, there are also some differences in the emission decay profile, particularly at short times after the laser pulse, possibly indicating a minor dynamic component in the quenching. The similarity in the temporal profiles beyond 0.1 μs indicates a predominantly static interaction for [Ru(bpy)$_3^{2+}$−TP$^+$]@Y. The significant decrease in emission intensity upon inclusion of TP$^+$ and the similar kinetic behavior of the residual emission both emphasize the static nature of the interaction. These observations are intuitively expected given that the interacting species are immobilized in separate zeolite cavities with no possibility of diffusion.

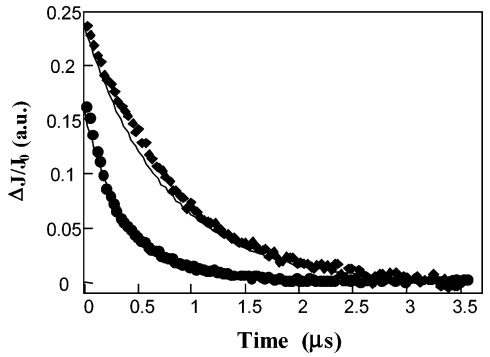

Figure 5. Emission decay monitored at 600 nm for Ru(bpy)$_3^{2+}$ (◆) and [Ru(bpy)$_3^{2+}$−TP$^+$]@Y (●) under N_2. The continuous lines correspond to the best fit of the experimental points.

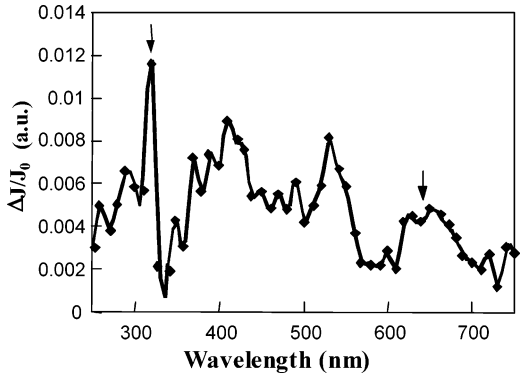

Figure 6. Transient diffuse reflectance UV−vis spectrum of [Ru(bpy)$_3^{2+}$−TP$^+$]@Y recorded 13.2 μs after 532-nm laser excitation. The peaks attributed to Ru(bpy)$_3^{3+}$ have been marked with an arrow.

Further information on TP$^+$ quenching of the Ru(bpy)$_3^{2+}$ triplet excited state was obtained by laser flash photolysis using 532 nm as the excitation wavelength. Wavelengths longer than 470 nm result in the preferential excitation of Ru(bpy)$_3^{2+}$, as demonstrated by the emission versus excitation wavelength map shown in Figure 3. Unfortunately, the transient spectrum after the laser pulse was too complex to be interpreted exhaustively. Among other features, this spectrum contains the bleaching due to the Ru(bpy)$_3^{2+}$ ground state as well as the absorption and emission from its excited state, species related to TP$^+$, and alkali metal ion clusters (Na_4^{3+}, for example).[14] Despite the complexity, at long time scales it is possible to recognize a sharp absorption at 310 nm as well as a broad band (600−700 nm) attributable to the Ru(bpy)$_3^{3+}$ complex (Figure 6).[51,52] No growth of the signals due to the formation of Ru(bpy)$_3^{3+}$ was observed, indicating that its generation must be instantaneous on the microsecond time scale. The Ru^{3+} complex is formed following electron transfer from the Ru(bpy)$_3^{2+}$ excited state to an electron acceptor. In the absence of TP$^+$, the transient absorption spectrum is dominated by Ru(bpy)$_3^{2+}$ emission, and the absorption band due to Ru(bpy)$_3^{3+}$ is not observed, confirming TP$^+$ as the electron-accepting species. The lifetime of photogenerated Ru(bpy)$_3^{3+}$ is longer than hundreds of microseconds, indicating that back electron transfer in [Ru(bpy)$_3^{3+}$−TP$^\bullet$]@Y is slow. Confirmation of the TP$^\bullet$ radical (λ_{max} 540 nm) is complicated because of the low extinction coefficient of this radical and the presence of many other absorptions and emissions in this spectral region. However, by combining the information from the emission and laser flash photolysis experiments, it can be concluded that approximately 70% of Ru(bpy)$_3^{2+}$ triplets are "instantaneously" quenched in the presence of TP$^+$.

The above results provide the basis for our investigations into the influence of the medium interposed between the donor and

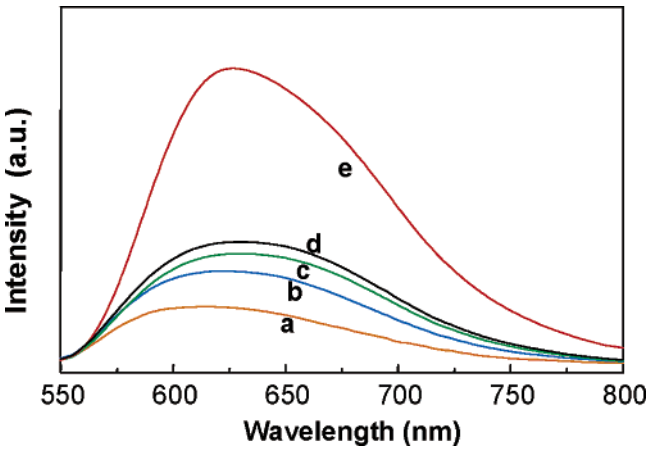

Figure 7. Average emission spectra (λ_{ex} = 466 nm) of samples (a) [Ru(bpy)$_3^{2+}$−TP$^+$]@Y, (b) [Ru(bpy)$_3^{2+}$−TiO$_2$(0.9)−TP$^+$]@Y, (c) [Ru(bpy)$_3^{2+}$−TiO$_2$ (1.8)−TP$^+$]@Y, (d) [Ru(bpy)$_3^{2+}$−TiO$_2$]@Y, and (e) Ru(bpy)$_3^{2+}$@Y. Each of these spectra is an average of nine independent measurements.

acceptor. The following data are for [Ru(bpy)$_3^{2+}$−TP$^+$]@Y samples incorporating semiconductor metal oxide clusters (TiO$_2$). Two samples, differing in the final TiO$_2$ loading, were prepared (Table 1). As a control, [Ru(bpy)$_3^{2+}$−TiO$_2$]@Y (TP$^+$ is absent) was also studied. Diffuse reflectance UV−vis spectroscopy of [Ru(bpy)$_3^{2+}$−TiO$_2$−TP$^+$]@Y indicates the presence of TiO$_2$ clusters by and increased absorption in the 200−250-nm region of the spectrum. FT-Raman spectroscopy serves to monitor the transformation of monomeric Ti═O^{2+} (530 cm^{-1}) into oligomeric TiO$_2$ with anatase-like structure (394, 517, and 637 cm^{-1}). The rationale behind the co-encapsulation of TiO$_2$ was to examine its behavior as an electron relay or molecular wire, promoting a more efficient movement of electrons with respect to the situation in which the donor and the acceptor encapsulated in the zeolitic medium do not have any interposed TiO$_2$. It has to be considered that modeling at the AM1 level shows that the maximum number of Ti atoms that can be allocated in a zeolite Y cavity is about 16 and that the properties of such small TiO$_2$ clusters are different from those measured for typical TiO$_2$ standards.

Emission spectra of the two [Ru(bpy)$_3^{2+}$−TiO$_2$−TP$^+$]@Y samples were recorded under the same conditions as previously used and were compared to spectra of Ru(bpy)$_3^{2+}$@Y, [Ru(bpy)$_3^{2+}$−TP$^+$]@Y, and [Ru(bpy)$_3^{2+}$−TiO$_2$]@Y as references to determine the influence of TiO$_2$ in the system. It was observed that whereas 70% of Ru(bpy)$_3^{2+}$ emission is quenched by TP$^+$ the presence of TiO$_2$ partially restores the initial emission intensity. This increase is proportional to the titanium content (Figure 7). Thus, the TP$^+$ quenching of Ru(bpy)$_3^{2+}$ emission is impeded to a significant degree by the presence of TiO$_2$, and the emission of [Ru(bpy)$_3^{2+}$−TiO$_2$−TP$^+$]@Y approaches 90% of the value measured for the binary system, [Ru(bpy)$_3^{2+}$−TiO$_2$]@Y. The latter sample represents the extreme case where, obviously, there is no interaction between Ru(bpy)$_3^{2+}$ and TP$^+$. The compiled evidence indicates that small TiO$_2$ clusters encapsulated within zeolite Y disfavors the donor−acceptor interaction in this system, behaving as an insulator.

Efficient photoinduced electron transfer between Ru(bpy)$_3^{2+}$ complexes adsorbed on TiO$_2$ particles (∼50 nm) has been extensively demonstrated and is the basis of dye-sensitized solar cells. However, as the particle size decreases below the quantum size, the band gap is known to increase. This effect is also clearly observed for encapsulated TiO$_2$, for which the band gap shifts significantly to 3.6 eV that is very different from the 3.2 eV characteristic of TiO$_2$ standard. In contrast, the photophysical properties of Ru(bpy)$_3^{2+}$ are similar in solution than in zeolites. Thus, our study shows that as a consequence of the band gap increase and the shifts of the conduction band of encapsulated TiO$_2$, the electron transfer between Ru(bpy)$_3^{2+}$ and TiO$_2$ may not be as favorable as for nanometric particles.

However, previous studies by us[30] and other groups[12,50] have shown that the apparent photocatalytic activity of encapsulated Ru(bpy)$_3^{2+}$ increases upon codoping by TiO$_2$. The system reported here is somewhat different because the donor and the acceptor are simultaneously immobilized inside the zeolite cavities and the effect of interposed TiO$_2$ refers to the comparison between direct or relayed electron transfer.

In conclusion, this work demonstrates that immobilized Ru(bpy)$_3^{2+}$ and TP$^+$ are capable of efficient through-space electron transfer even when segregated in separate zeolite cavities. This electron-transfer interaction can be disfavored by the medium interposed between the two ions. Semiconductor oxide TiO$_2$ was shown to disrupt this interaction significantly. These results exemplify how the rigid, compartmentalized space provided by the zeolite host can serve to build and maintain spatially arranged multicomponent systems, in which a modulation of the donor−acceptor interaction can be accomplished.

Experimental Section

The sample of Ru(bpy)$_3^{2+}$@Y was obtained by ion exchange of a commercial NaY sample (Aldrich LYZ-53) using a dilute aqueous solution of [Ru(NH$_3$)$_6$]Cl$_3$, followed by the addition of excess bipyridine and heating under vacuum at 200 °C for 24 h. The Ru(bpy)$_3^{2+}$@Y sample was submitted to exhaustive solid−liquid extraction for 2 weeks according to the method originally reported by Herron.[31,32,53]

[Ru(bpy)$_3^{2+}$−TP$^+$]@Y was prepared from Ru(bpy)$_3^{2+}$@Y (thermally dehydrated at 110 °C for 4 h) by the addition of this zeolite (1 g) to a solution of 1,3,5-triphenyl-2-penten-1,5-dione (0.16 mmol) in CH$_2$Cl$_2$ (5 mL). The suspension was refluxed under continuous stirring for 2 h. After this time, the solid was collected by filtration and baked at 110 °C for 2h.

The samples containing TiO$_2$ were prepared by stirring suspensions of the appropriate material, Ru(bpy)$_3^{2+}$@Y or [Ru(bpy)$_3^{2+}$−TP$^+$@Y], for 5 h at room temperature in aqueous solutions containing (NH$_4$)$_2$(Ti═O)(C$_2$O$_4$)$_2$·H$_2$O at various concentrations (0.2 or 0.4 M) in a solid−liquid ratio of 0.1. This was followed by mild baking at 150 °C according to the reported procedure.[54,55]

FT-IR spectra were recorded using a Nicolet 710 FT spectrophotometer. Self-supported zeolite wafers (∼10 mg) were compressed at 1 ton cm^{-2} for 3 min and placed in sealed greaseless cells with CaF$_2$ windows. The cells were outgassed at 200 °C under 10^{-2} Pa for 1 h before recording the spectrum at room temperature. DR-UV−vis spectra were recorded with a Cary 5G spectrophotometer using a praying mantis attachment and BaSO$_4$ as a reference. Steady-state emission spectra were recorded at room temperature in an Edinburgh FL900 spectrofluorimeter. The excitation wavelength was varied every 10 nm from 420 to 490 nm. The zeolites as powder samples were placed in septum-capped Suprasil quartz cells and purged with nitrogen for at least 15 min prior to recording the emission. The spectra were recorded under the same conditions, nine times on different days and in different order. The average of these nine independent measurements was considered to be the legitimate emission of each sample. No significant deviation in the relative emission intensity for the samples was observed for each individual set of measurements.

Time-resolved DR-UV−vis measurements were made using the second (532 nm) or third (355 nm) harmonic pulse of a Surelite Nd:YAG laser ($\leq$10 ns pulse width; $\leq$20 mJ pulse^{-1}) as the excitation source. Signals from the photomultiplier tube were captured and digitized by a Tektronix 2440 transient digitizer and transferred to a Power Macintosh programmed in the LabView environment. Details of similar time-resolved diffuse reflectance systems have been described elsewhere.[56−58] Samples were irradiated in 3 $\times$ 7 mm^2 Suprasil quartz cells and were purged with nitrogen for at least 30 min prior to each experiment.

Acknowledgment. Financial support by the Spanish DGICYT (H.G., MAT2003-1672) and Canadian NSERC through an operating grant (J.C.S.) is gratefully acknowledged. M.N.C. thanks the Ontario Graduate Scholarship Program and NSERC for postgraduate scholarships.

References and Notes

(1) Scaiano, J. C.; García, H. *Acc. Chem. Res.* **1999**, *32*, 783.
(2) Yoon, K. B.; Hubig, S. M.; Kochi, J. K. *J. Phys. Chem.* **1994**, *98*, 3865.
(3) Garcia, H.; Roth, H. D. *Chem. Rev.* **2002**, *102*, 3947.
(4) Tung, C. H.; Wu, L. Z.; Zhang, L. P.; Chen, B. *Acc. Chem. Res.* **2003**, *36*, 39.
(5) Lee, H.; Dutta, P. K. *J. Phys. Chem. B* **2002**, *106*, 11898.
(6) Ranjit, K. T.; Kevan, L. *J. Phys. Chem. B* **2002**, *106*, 9306.
(7) Park, Y. S.; Lee, E. J.; Chun, Y. S.; Yoon, Y. D.; Yoon, K. B. *J. Am. Chem. Soc.* **2002**, *124*, 7123.
(8) Moissette, A.; Vezin, H.; Gener, I.; Patarin, J.; Bremard, C. *Angew. Chem., Int. Ed.* **2002**, *41*, 1241.
(9) Ranjit, K. T.; Kevan, L. *J. Phys. Chem. B* **2002**, *106*, 1104.
(10) O'Neill, M. A.; Cozens, F. L.; Schepp, N. P. *J. Phys. Chem. B* **2001**, *105*, 12746.
(11) Castagnola, N.; Dutta, P. K. *Stud. Surf. Sci. Catal.* **2001**, *135*, 4508.
(12) Bossmann, S. H.; Turro, C.; Schnabel, C.; Pokhrel, M. R.; Payawan, L. M., Jr.; Baumeister, J. B.; Wörner, M. *J. Phys. Chem. B* **2001**, *105*, 5374.
(13) Kincaid, J. R. *Chem.—Eur. J.* **2000**, *6*, 4055.
(14) Brancaleon, L.; Brousmiche, D.; Rao, V. J.; Johnston, L. J. *J. Am. Chem. Soc.* **1998**, *120*, 4926.
(15) Adam, W.; Corma, A.; Miranda, M. A.; Sabater-Picot, M. J.; Sahin, C. *J. Am. Chem. Soc.* **1996**, *118*, 2380.
(16) Krüger, J. S.; Mayer, J. E.; Mallouk, T. E. *J. Am. Chem. Soc.* **1988**, *110*, 8232.
(17) Brigham, E. S.; Snowden, P. T.; Kim, Y. I.; Mallouk, T. E. *J. Phys. Chem.* **1993**, *97*, 8650.
(18) Dutta, P. K.; Turbeville, W.; Robins, D. S. *J. Phys. Chem.* **1992**, *96*, 5024.
(19) Kim, Y. I.; Mallouk, T. E. *J. Phys. Chem.* **1992**, *96*, 2879.
(20) Sankararaman, S.; Yoon, K. B.; Yabe, T.; Kochi, J. K. *J. Am. Chem. Soc.* **1991**, *113*, 1419.
(21) Dutta, P. K.; Das, S. K. *J. Am. Chem. Soc.* **1997**, *119*, 4311.
(22) Countant, M. A.; Le, T.; Castagnola, N.; Dutta, P. K. *J. Phys. Chem. B* **2000**, *104*, 10783.
(23) Kim, Y. I.; Keller, S. W.; Krueger, J. S.; Yonemoto, E. H.; Saupe, G. B.; Mallouk, T. E. *J. Phys. Chem. B* **1997**, *101*, 2491.
(24) De Wilde, W.; Peeters, G.; Lunsford, J. H. *J. Phys. Chem.* **1980**, *84*, 2306.
(25) Sykora, M.; Kincaid, J. R.; Dutta, P. K.; Castagnola, N. B. *J. Phys. Chem. B* **1999**, *103*, 309.
(26) Sykora, M.; Maruszewski, K.; Treffet, Z.; Shelly, M.; Kincaid, J. R. *J. Am. Chem. Soc.* **1998**, *120*, 3490.
(27) Sykora, M.; Kincaid, J. R. *Nature* **1997**, *387*, 162.
(28) Borja, M.; Dutta, P. K. *Nature* **1993**, *362*, 43.
(29) Bossmann, S. H.; Herrmann, D.; Braun, A. M.; Turro, C. *J. Inf. Rec.* **1998**, *24*, 271.
(30) Cosa, G.; Chretien, M. N.; Galletero, M. S.; Fornes, V.; Garcia, H.; Scaiano, J. C. *J. Phys. Chem. B* **2002**, *106*, 2460.
(31) Herron, N.; Stucky, G. D.; Tolman, C. A. *J. Chem. Soc., Chem. Commun.* **1986**, 1521.
(32) Herron, N. *Inorg. Chem.* **1986**, *25*, 4714.
(33) Lunsford, J.; De Wilde, W.; Peeters, G. *J. Phys. Chem.* **1980**, *84*, 2306.
(34) Corma, A.; Fornés, V.; García, H.; Miranda, M. A.; Primo, J.; Sabater, M. J. *J. Am. Chem. Soc.* **1994**, *116*, 2276.
(35) Lunsford, J. *ACS Symp. Ser.* **1977**, *40*, 473.
(36) Corma, A.; Fornés, V.; García, H.; Miranda, M. A.; Sabater, M. J. *J. Am. Chem. Soc.* **1994**, *116*, 9767.
(37) Liu, X.; Iu, K. K.; Thomas, J. K. *J. Chem. Soc., Faraday Trans.* **1993**, *89*, 1861.
(38) Grubert, G.; Wark, M.; Jaeger, N. I.; Schulz-Ekloff, G. *J. Phys. Chem. B* **1998**, *102*, 1665.
(39) Klass, J.; Schulz-Ekloff, G.; Jaeger, N. I. *J. Phys. Chem. B* **1997**, *101*, 1305.
(40) Corrent, S.; Cosa, G.; Scaiano, J. C.; Galletero, M. S.; Alvaro, M.; García, H. *Chem. Mater.* **2001**, *13*, 715.
(41) Anpo, M.; Ichihashi, Y.; Takeuchi, M.; Yamashita, H. *Res. Chem. Intermed.* **1998**, *24*, 143.
(42) Cardin, D.; Constantine, S.; Gilbert, A.; Lay, A.; Galletero, M. S.; Alvaro, M.; García, H.; Márquez, F. *J. Am. Chem. Soc.* **2001**, *123*, 3141.
(43) Pereira, C.; Kokotailo, G. T.; Gorte, R. J. *J. Phys. Chem.* **1991**, *95*, 705.
(44) Bein, T. In *Recent Advances and New Horizons in Zeolite Science and Technology*; Chon, H., Woo, S. I., Park, S.-E., Eds.; Studies in Surface Science and Catalysis; Elsevier: Amsterdam, 1996; Vol. 102; p 295.
(45) Lewis, F. J.; Barancyk, S. V.; Burch, E. L. *J. Am. Chem. Soc.* **1992**, *114*, 3866.
(46) Millar, G. J.; Lewis, A. R.; Bowmaker, G. A.; Cooney, R. P. *J. Mater. Chem.* **1993**, *3*, 867.
(47) Bordiga, S.; Ricchiardi, G.; Spoto, G.; Scarano, D.; Carnelli, L.; Zecchina, A.; Arean, C. O. *J. Chem. Soc., Faraday Trans.* **1993**, *89*, 1843.
(48) Galletero, M. S.; Alvaro, M.; Garcia, H.; Gomez-Garcia, C. J.; Lay, A. K. *Phys. Chem. Chem. Phys.* **2002**, *4*, 115.
(49) Dutta, P. K.; Incavo, J. A. *J. Phys. Chem.* **1987**, *91*, 4443.
(50) Kim, Y. I.; Keller, S. W.; Krüger, J. S.; Yonemoto, E. H.; Saupure, G. B.; Mallouk, T. E. *J. Phys. Chem. B* **1997**, *101*, 2491.
(51) Corma, A.; Fornes, V.; Galletero, M. S.; Garcia, H.; Scaiano, J. C. *Chem. Commun.* **2002**, 334.
(52) Lomoth, R.; Haupl, T.; Johansson, O.; Hammarstrom, L. *Chem.—Eur. J.* **2002**, *8*, 102.
(53) Ha, J.-H.; Jung, G. Y.; Kim, M.-S.; Lee, Y. H.; Shin, K.; Kim, Y.-R. *Bull. Korean Chem. Soc.* **2001**, *22*, 63.
(54) Liu, X.; Iu, K. K.; Thomas, J. K. *J. Chem. Soc., Faraday Trans.* **1993**, *89*, 1861.
(55) Cosa, G.; Galletero, M. S.; Fernandez, L.; Marquez, F.; Garcia, H.; Scaiano, J. C. *New J. Chem.* **2002**, *26*, 1448.
(56) Wilkinson, F.; Willsher, C. *J. Appl. Spectrosc.* **1984**, *38*, 897.
(57) Wilkinson, F.; Kelly, G. Diffuse Reflectance Flash Photolysis. In *Handbook of Organic Photochemistry*; Scaiano, J. C., Ed.; CRC Press: Boca Raton, FL, 1989; Vol. 1, p 293.
(58) Scaiano, J. C.; Tanner, M.; Weir, D. *J. Am. Chem. Soc.* **1985**, *107*, 4396.